Neuroinform (2009) 7:195–210
DOI 10.1007/s12021-009-9052-3

NETMORPH: A Framework for the Stochastic Generation of Large Scale Neuronal Networks With Realistic Neuron Morphologies

Randal A. Koene · Betty Tijms · Peter van Hees · Frank Postma · Alexander de Ridder · Ger J. A. Ramakers · Jaap van Pelt · Arjen van Ooyen

Published online: 12 August 2009

Abstract We present a simulation framework, called NETMORPH, for the developmental generation of 3D large-scale neuronal networks with realistic neuron morphologies. In NETMORPH, neuronal morphogenesis is simulated from the perspective of the individual growth cone. For each growth cone in a growing axonal or dendritic tree, its actions of elongation, branching and turning are described in a stochastic, phenomenological manner. In this way, neurons with realistic axonal and dendritic morphologies, including neurite curvature, can be generated. Synapses are formed as neurons grow out and axonal and dendritic branches come in close proximity of each other. NETMORPH is a flexible tool that can be applied to a wide variety of research questions regarding morphology and connectivity. Research applications include studying the complex relationship between neuronal morphology and global patterns of synaptic connectivity. Possible future developments of NETMORPH are discussed.

Keywords Neurite outgrowth · Growth model · Growth cone · Morphogenesis · Synaptic connectivity · Neural networks · Neural development

R. A. Koene · B. Tijms · P. van Hees · F. Postma · A. de Ridder · J. van Pelt · A. van Ooyen (✉)
Department of Integrative Neurophysiology,
Center for Neurogenomics and Cognitive Research,
VU University Amsterdam,
De Boelelaan 1085,
1081 HV Amsterdam, the Netherlands
e-mail: arjen.van.ooyen@cncr.vu.nl

G. J. A. Ramakers
Netherlands Institute for Neuroscience,
Meibergdreef 47,
1105 BA Amsterdam, the Netherlands

Introduction

Activity dynamics in neuronal networks depends to a large extent on the pattern of synaptic connections between neurons (Douglas and Martin 2004). Because the formation of synapses requires overlap between axons and dendrites, neuronal morphology is an important determinant of network connectivity. Neurons develop their characteristic morphology of branched axons and dendrites by way of the dynamic behavior of growth cones—specialized structures at the ends of outgrowing neurites that mediate neurite elongation and branching (Letourneau et al. 1991). Synapses can occur where axonal and dendritic branches of different neurons come sufficiently close to each other (Braitenberg and Schütz 1998; Peters 1979). The resulting local and global patterns of synaptic connectivity (e.g., connection length distribution; "small-world" properties; Sporns et al. 2004) that emerge during development will depend on the specific characteristics of axonal and dendritic arbors, such as their length, number of segments, branching structure and coverage of space. In general, however, it is not well understood how these details of neuronal morphology and the local processes of neurite outgrowth and synapse formation influence global connectivity. To be able to investigate such issues as the formation of synaptic connectivity during development and the relationship between neuronal morphology and synaptic connectivity, we need a simulation framework that can generate large scale networks with realistic neuronal morphologies by using outgrowth rules for axons and dendrites.

In this paper, we present a simulation framework, called NETMORPH, for the stochastic and developmental generation of 3D large scale neuronal networks with realistic neuronal morphologies. In our framework, neuronal mor-

phogenesis is simulated from the perspective of the individual growth cone. The various actions of the growth cone, such as elongation, branching and turning, are described as outcomes of stochastic processes that capture in a phenomenological manner the processes involved in neurite outgrowth. This description includes the influence on outgrowth of the growth cone's position in the growing tree and of competition for resources between different growth cones of a dendrite or an axon. The model for 3D neuronal morphogenesis is based on the dendritic growth model of Van Pelt et al., (Van Pelt et al. 2001a; Van Pelt and Uylings 2002, 2003, 2005) and extended with rules for the direction of neurite outgrowth and branching angles. Synapses are formed as neurons grow out, and are determined on the basis of proximity between axonal and dendritic branches.

The many applications of our framework include creating detailed network connectivity patterns, with axo-dendritic synapses at specific locations in the neuronal morphology; studying how typical connectivity patterns come about during development (e.g., small-world connectivity; Sporns et al. 2004); examining how characteristic changes in synaptic connectivity, as observed in brain diseases such as Alzheimer's disease and autism, may arise from alterations in neuronal morphology (Belmonte and Bourgeron 2006; Scheff et al. 2007); and investigating the complex relationship between neuronal morphology and local and global patterns of synaptic connectivity. The neuronal morphologies and synaptic connectivities as produced by NETMORPH could also be made available to tools such as NEURON to simulate activity dynamics.

Other simulators for generating neuronal network structures exist, but they differ with respect to the temporal aspects of neuronal development, the morphology of single neurons, or the connectivity in the generated networks. The modeling tool neuroConstruct (Gleeson et al. 2007) for creating neuronal networks in 3D space requires neuronal morphologies to be imported or specified, but it cannot grow the morphologies using developmental rules for neurite elongation and branching. The simulator L-Neuron is designed to create virtual neurons that are anatomically indistinguishable from their real counterparts using an L-systems approach by means of iteratively sampling experimental distributions of neuronal shape parameters (Senft and Ascoli 1999; Ascoli and Krichmar 2000; Ascoli et al. 2001a, b; Samsonovich and Ascoli 2007). Similarly, the simulator tool NeuGen (Eberhard et al. 2006) generates neuronal networks in 3D with morphologically realistic neurons by sampling experimental distributions of morphological shape parameters. Recently, Luczak (2006) showed how basic environmental factors and simple rules of diffusive growth already adequately account for the spatial embedding of tree structures of cortical dendrites. A new computer package that is currently under development is CX3D for the simulation of cortical development in 3D space, including the morphology of single neurons (Zubler and Douglas 2008).

Only few models exist that describe the development of network connectivity. Van Ooyen et al. used models in which the morphology of a single neuron was represented in a highly abstract manner (Van Ooyen and Van Pelt 1994, 1996; Van Ooyen et al. 1995, 1996). In their approach, growing neurons were modeled as expanding, circular neuritic fields, without a distinction between axons and dendrites. A similar and still very abstract approach, but using separate axonal and dendritic processes, is taken by Butz et al. (2006). Segev and Ben-Jacob (2000) provide a model for the self-wiring of neuronal networks based on chemotaxis. Their model contains migrating growth cones without detailed neuronal morphology.

The structure of the article is as follows. Section 2 describes general aspects of the modeling approach. Section 3 covers the structure of, and the assumptions underlying, the model for neurite outgrowth and branching. Section 4 concentrates on parameter optimization, the use of the simulator, and model validation through comparisons with experimental data. Section 5 describes the model for locating candidate synapses and the emerging connectivity in the network. Section 6 deals with some implementation issues and the use of the simulator NETMORPH. The paper ends with a Discussion, in which we outline some future extensions of NETMORPH.

Modeling Considerations

Choice of Model

Growth cones exhibit complex behavior, as outcomes of a multitude of intracellular processes and chemical and structural interactions with their local environments (Bamburg 2003; Goldberg and Burmeister 1989). These intra- and extracellular mechanisms can cause a growth cone: (a) to start or to stop extending, or even to retract, (b) to bifurcate (branch), and (c) to change direction (turn) (Isbister and O'Connor 1999; Polinsky et al. 2000). In describing growth cone behavior one needs to make choices for the level of granularity, which can range from the phenomenological level of minimal assumptions up to highly detailed descriptions of biophysical processes underlying the dynamic behavior of growth cones and outgrowing neurites (e.g., Goodhill 1998; Hentschel and Van Ooyen 1999; Aeschlimann 2000; Graham and Van Ooyen 2004; Hely et al. 2001; Maskery et al. 2004; Kiddie et al. 2005). In NETMORPH, the neurite outgrowth and branching models are based on existing phenomenological dendritic growth models as formulated by Van Pelt and

co-workers (e.g., Van Pelt and Uylings 2003; Van Ooyen and Van Pelt 1994). These models take a stochastic approach based on simple rules (functions) for neurite branching and elongation. They have been validated for a variety of neuronal cell types and have been demonstrated to accurately describe the dendritic metrical and topological variability within and between cell types (e.g., Van Pelt et al. 2001a, b). In NETMORPH we extended and modified these models in order to simulate (i) growth in 2D or 3D, (ii) growth of axons and dendrites, and (iii) neurite curvature (tortuosity).

Discretization of Time

A discretization of time is used in NETMORPH, whereby during each time interval Δt, a growth cone may (i) migrate, so that the trailing neurite is elongated; (ii) bifurcate, resulting in two daughter growth cones (and branches); and (iii) change direction, so that a turn appears in the neurite. The processes involved in neurite outgrowth may all have characteristic but different time scales. Adapting the size of the time steps to a slow process may implicate inappropriate treatment of fast mechanisms. Alternatively, adapting the time steps to fast processes may imply inaccurate simulation of slow processes due to oversampling. In its present implementation, NETMORPH uses fixed time steps with probabilistic functions for elongation and branching. The growth model of Van Pelt et al. was developed with the condition that branching probabilities per time step are small (<<1), in order to neglect the possible occurrence of more than one branching event at a growth cone per time step. This condition places an upper limit on the size of the time step. Elongation is treated with a more coarse-grained time division. To include variability on this coarser time scale, we randomly assign an elongation rate to a newly formed growth cone (i.e., at a branching event) for the period up to the next branching event of the growth cone.

Space

There is no discretization of space in NETMORPH. Separate simulation programs, NETMORPH and NETMORPH2D, are provided for three dimensional and exclusively two dimensional simulations, respectively. Space can be bounded explicitly to force the outgrowing neurites to stay within these bounded regions.

Modeling Neuronal Morphogenesis

The Van Pelt growth model describes neuronal outgrowth as a stochastic process in time in which neurites can elongate and bifurcate. The model defines the probabilities per time step of these actions as functions of time. The model is designed to be as simple as possible and, although phenomenological in nature, is inspired by actual biological processes underlying neurite outgrowth. Basic assumptions include that (i) all the tips (i.e., growth cones) of a neuronal tree are assumed to participate in the branching and elongation process, (ii) neurite elongation reflects the final outcome of a process of outgrowth and retraction, and (iii) branching and elongation are modeled as independent processes. This last assumption implies that the validation of the model can proceed in separate phases, with first validating the branching process and then the elongation process. Note that length characteristics of a tree depend on the properties of both the branching and the elongation process.

Branching Probability

The probability per unit of time of a branching event at a given terminal segment j (i.e., growth cone) is given by (e.g. Van Pelt and Uylings 2002, 2003, 2005, 2007)

$$p_j(t|n(t),\gamma) = D(t)n(t)^{-E}2^{-S\gamma_j}/C(t) \quad (1)$$

with

$$C(t) = \frac{1}{n(t)}\sum_{k=1}^{n(t)} 2^{-S\gamma_k}.$$

The time-dependent branching probability p_j of a given terminal segment j is composed of three terms: a baseline branching rate function $D(t)$; a term $n(t)^{-E}$ making the branching probability dependent on the momentary total number of terminal segments, $n(t)$, in the tree, with a free 'competition' parameter E; and a term $2^{-S\gamma_j}/C(t)$ making the branching probability dependent on the centrifugal order γ_j of the terminal segment (i.e. its position in the tree; see Fig. 1a). The terms $2^{-S\gamma_k}$ are weight factors modulated by the free parameter S, and assigned to all terminal segments, normalized by the mean weight $C(t)$. The function $D(t)$ is an 'a priori' unknown function representing all factors involved in branching not covered by the 2nd and 3rd term in (1). The 3rd term modulates the branching probabilities according to the position of the terminal segments in the tree. For $S=0$, all terminal segments have equal branching probabilities. For $S>0$, proximal terminal segments (relative to the root) bifurcate with higher probabilities than distal ones, while for $S<0$, distal terminal segments bifurcate with higher probabilities than proximal ones. Parameter S uniquely determines the topological asymmetry of the generated trees (Van Pelt et al. 1992).

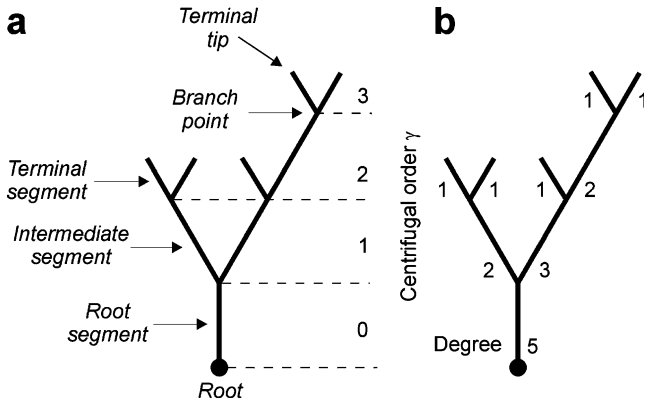

Fig. 1 (**a**) Elements of a topological tree; the segments are labeled according to their centrifugal order γ. (**b**) Segment labeling according to degree (number of terminal segments of the subtree emerging from a segment)

The baseline branching rate function *D(t)* is approximated by an exponential function

$$D(t) = ce^{-t/\tau} \tag{2}$$

with time constant τ. Such a function was necessary to match the shape of the experimental growth curve of the increasing number of dendritic terminal segments during outgrowth of rat cortical multipolar nonpyramidal cells (Van Pelt and Uylings 2003). An important parameter is the time integral *B(t)* of the function *D(t)* over the period of growth

$$B(t) = \int_0^t D(s)ds = \int_0^t ce^{-s/\tau}ds \tag{3}$$

denoting the expected number of branching events at an isolated segment (or for E=0) in the period of growth. By using the asymptotic value for *B(t)* we obtain:

$$\begin{aligned} B_\infty &= B(\infty) = c\tau \\ B(t) &= B_\infty\left(1 - e^{-t/\tau}\right) \end{aligned} \tag{4}$$

As discussed above, neurite outgrowth is implemented in NETMORPH on a discrete time scale, with fixed time steps of duration Δt. The probability of branching of a terminal segment j in time step $(t_i, t_i + \Delta t)$ then becomes

$$p_{i,j} = D_i n_i^{-E} 2^{-S\gamma_j} / C_{n_i} \tag{5}$$

with n_i the number of terminal segments in time step i and D_i defined as

$$D_i \int_{t_i-\Delta t}^{t_i} D(t)dt = B(t_i) - B(t_i - \Delta t) = B_\infty e^{-t_i/\tau}\left(e^{\Delta t/\tau} - 1\right) \tag{6}$$

resulting in the expression

$$p_{i,j} = n_i^{-E} B_\infty e^{-t_i/\tau}\left(e^{\Delta t/\tau} - 1\right)2^{-S\gamma_j} / C_{n_i} \tag{7}$$

again with

$$C_{n_i} = \frac{1}{n_i}\sum_{k=1}^{n_i} 2^{-S\gamma_k}$$

The branching process of a tree is thus fully defined by the parameters B_∞, E, S, τ, and the period of growth T. Examples of optimized values for these parameters for a variety of cell types are summarized in Van Pelt et al. (2001b).

Elongation

The rate of elongation of a growth cone may vary considerably (e.g., Lamoureux et al. 1998; da Costa et al. 2002), also on the time scale of the chosen time steps Δ*t*. In NETMORPH a more coarse grained approach is used by taking an averaged elongation rate for the period in which a terminal segment is elongating up to the occurrence of its next branching event. The daughter segments emerging from a branching event are then subsequently given an elongation rate up to their next branching events. NETMORPH assigns the elongation rates by randomly sampling a Gaussian distribution.

Alternatively, NETMORPH includes the option to select an elongation competition model. In addition to influencing branching probability, competition between growth cones for limited resources may also affect elongation rate (see also Van Ooyen et al. 2001), which can be described as

$$v(t) = v_0 n(t)^{-F} \tag{7a}$$

with parameter F determining the strength of competition (Van Pelt and Uylings 2003). For $F = 0$, terminal segments elongate with rate v_0 independent of the number of terminal segments. For $F > 0$, elongation rates depend on the momentary number of terminal segments. For $F = 1$, elongation rates are inversely correlated with the number of terminal segments, implying that the total tree increases its length with rate v_0.

Initial Length

Following a branching event, the daughter segments proceed in their outgrowth by elongation and possibly a further branching event. When a branching event occurs shortly after the previous one, a very short intermediate segment is produced. A random branching process results in an exponentially decreasing intermediate segment length distribution (Van Veen and Van Pelt 1993). Experimental data of intermediate segment lengths, however, show distributions with clear modal shapes (e.g., Nowakowski et al. 1992; Uylings et al. 1978, 1994). Apparently, short intermediate segments in dendritic reconstructions do occur much less frequently than expected. A possible explanation

is that the branching process of a real growth cone proceeds over a certain period of time, while it is treated in the model as a point process in time. To account for this observation, it is assumed in the model that the daughter branches already appear with a certain initial length (see also Van Pelt and Uylings 2007). This additional assumption resulted in accurate reproductions of the observed intermediate segment length distributions (Van Pelt et al. 2001a, b, 2003).

Direction of Outgrowth

The direction of outgrowth of a growth cone depends on many intracellular and extracellular cues, which may cause large fluctuations in outgrowth directions. The neurite segments from reconstructed neurons indeed show many deviations from a straight line at a range of spatial scales. NETMORPH includes the simulation of these morphological details, not only because they are highly characteristic of the visual appearance of a neuron, but also because they define how space is invaded by the axonal and dendritic arborizations. These morphological details influence the probability that axons and dendrites come into close proximity of each other, which is a prerequisite for the formation of synaptic connections (see Section 5).

In NETMORPH it is assumed that fluctuations in the direction of outgrowth of an individual neurite may occur at a time scale of the individual time steps Δt. It is further assumed that the new outgrowth direction depends on previous outgrowth directions and on a random component (see also Maskery et al. 2004).

Implementation The probability that growth cones change their direction of outgrowth during the interval $(t_i, t_i + \Delta t)$ is determined independently of the branching probability. At each growth cone j, the probability of a change in direction in time interval $(t_i, t_i + \Delta t)$ is given by

$$P_d(t_i) = r_L \Delta L_j(t_i) \tag{8}$$

where the rate parameter r_L (turns/μm) relates the elongation $\Delta L_j\,(t)$ of a terminal segment with the probability $P_d(t)$ that a change in direction occurred during the update interval. For each growth cone, NETMORPH decides that a direction change has occurred if $X < P_d(t)$, where $X \in [0, 1]$ has a uniform distribution. As long as no change occurs the piece of neurite keeps elongating in the same direction. When a change occurs the new direction is calculated and the propagation subsequently takes place in that direction. With this approach a neuritic segment consists of a series of straight segment pieces.

History-Weighted Direction of Outgrowth For the calculation of a new direction of outgrowth the orientations of previous segment pieces are taken into account based on the assumption that the stiffness of neuritic segments, which creates a force, restricts the new orientations of neurite outgrowth. Stiffness of neuritic segments increases when microtubule associated proteins (e.g., MAP2) bind to the microtubule cytoskeleton, which also gives rise to longer microtubule polymers (e.g., Sanchez et al. 2000; Kowalski and Williams 1993). The new direction is obtained by assigning weight factors to the previous orientations and taking the vector sum of these weighted orientations. This sum vector is finally perturbed by a random deviation, resulting in a new direction of outgrowth (Fig. 2):

$$\mathbf{d} = \sum\nolimits_k W_k \mathbf{u}_k + \mathbf{r}_\alpha \tag{9}$$

The summation takes into account past segment pieces from the last bifurcation point onward, whose orientations are given by the unit vectors $\mathbf{u}_k$. The weight factor W_k of a segment piece k is taken as $W_k = M_k / D_k^p$, with M_k the volume of the segment (or length if no segment diameter is specified), and D_k the distance from the segment's center along the neurite path to the elongating tip. The free parameter p is an exponent determining the dependence on history. For $p = 0$ there is no distance dependence, for $p > 0$ the most recent segment pieces have more weight than 'older' segment pieces, while for $p < 0$ the older segment pieces dominate over recent ones. The perturbation $\mathbf{r}_\alpha$ is a rotation over an angle α randomly drawn from a uniform distribution over the interval $[\alpha_{\min}, \alpha_{\max}]$, with $\alpha_{\min}$ and $\alpha_{\max}$ freely selectable parameters.

Branching Angles

An important observation with respect to branching angles and direction of outgrowth after a bifurcation was made by Uylings and Smit (1975), who found that in reconstructed pyramidal cell dendritic trees, parent and daughter segments at a bifurcation lie predominantly in one plane. Assuming

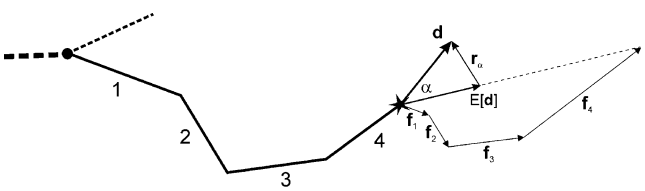

Fig. 2 Illustration in 2D of the calculation of the new outgrowth direction **d** with the *segment history tension* model. A history of 4 trailing segment pieces introduces 4 weighted direction vectors $\mathbf{f}_k$, whose vector summation results in vector $E[\mathbf{d}]$, via $E[\mathbf{d}] = \sum_k \mathbf{f}_k = \sum_k \left(M_k / D_k^p\right)\mathbf{u}_k$. Random perturbation in 2D over an angle α results in the actual outgrowth direction **d**

that this phenomenon is the result of forces exerted by the growth cones on the trailing neurites (e.g., Letourneau et al. 1991; Gordon-Weeks 2000; Kater and Guthrie 1990; see also Aeschlimann 2000) that stretch the parent and daughter segments into one plane, NETMORPH uses a *balance of forces* model to calculate the directions of outgrowth after a branching event.

Implementation At a branching event, forces are assigned to the daughter segments proportional to their initial lengths, and a branch angle β between the daughter segments is randomly drawn from a given PDF. A parallelogram is subsequently constructed resulting in a sum vector **d** (Fig. 3a), and its plane rotated such that the sum vector aligns with the orientation of the parent segment (Fig. 3b). Finally, the orientation of the plane of branching (in 3D) is rotated around the parent segment axis over an angle Ψ that is randomly drawn from a uniform distribution $[0, 2\pi]$.

Segment Diameters

A major determinant of the diameter of a dendritic segment is its microtubule cytoskeleton, which scales with the size of the dendritic tree emerging from the segment (Hillman 1979, 1988). Such scaling behavior becomes apparent at branch points where a parent segment with diameter d_p bifurcates into two daughter segments with smaller diameters d_1 and d_2. A power-law relation

$$d_p^e = d_1^e + d_2^e \tag{11}$$

(Rall 1959) is assumed between these diameters. Empirical values for the exponent e have been obtained for a variety of cell types (see overview in Van Pelt and Uylings (2005)). Because of the scaling behavior, a segment becomes thicker when the subtree it supports increases its number of terminal segments by ongoing branching. NETMORPH defines segment diameters at the end of the outgrowth process according to an iterative process described in Van Pelt and Uylings (2005). Briefly, terminal segment diameters are estimated by randomly sampling the observed terminal segment diameter distribution (or alternatively, a normal distribution with the observed mean-sd values). At each bifurcation, the diameter of the parent segment is estimated from its daughter segment diameters, by using a branch power value that is obtained from randomly sampling the observed branch power distribution.

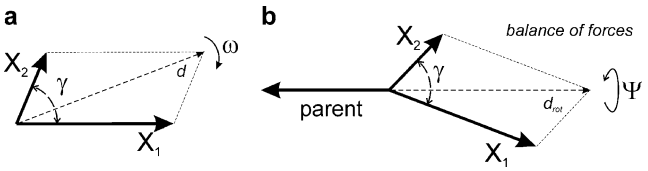

Fig. 3 (**a**) 'Forces' X_1 and X_2, and randomly selected branch angle β, drawn in a parallelogram construction to obtain the orientation of the sum vector **d**. (**b**) Rotation of the parallelogram such that the sum vector aligns with the orientation of the parent segment. The plane of branching is subsequently rotated (in 3D) around the axis of the parent segment by a uniformly random selected angle ψ in order to obtain the final orientations of the daughter segments

Validation and Use of the Model

Validation of the Model

The dendritic branching model has already been validated on a range of different cell types (Dityatev et al. 1995; Van Pelt et al. 1997), and a summary of optimized parameter values is given in Van Pelt et al. (2001b). The cell types analyzed include (i) basal dendrites of Wistar-rat cortical layer 5 large pyramidal neurons (Van Pelt and Uylings 2005), (ii) basal dendrites of Wistar-rat cortical layer 5 small pyramidal neurons (Van Pelt and Uylings 1999), (iii) basal dendrites of S1-rat cortical layer 2/3 pyramidal neurons (Van Pelt et al. 2001a), (iv) guinea pig cerebellar Purkinje cell dendritic trees (Van Pelt et al. 2001a), and (v) cat deep layer superior colliculus neurons (Van Pelt et al. 2001c). Diameter parameters for cell types (i) and (ii) were obtained from Larkman (1991) and Larkman et al. (1992), for cell type (iii) from Hillman (1988) and Larkman (1991), for cell type (iv) from Hillman (1988), and for cell type (v) from Schierwagen and Grantyn (1986). Figure 4 shows an example of how model neurons and experimentally reconstructed neurons match in the morphology of their dendrites, with respect to distributions of a number of shape properties.

The Sholl method was used to validate the 3D embedding of the neuronal branching patterns (Fig. 5). The 'experimental' Sholl curve was calculated for the basal dendrites of reconstructed day 13 rat cortical layer 2/3 pyramidal neurons taken from the Markram data set at Neuromorpho.org. The 'model' Sholl curve was calculated for a set of NETMORPH generated dendrites based on a parameter set optimized for the 3D data set of day 18 rat cortical layer 2/3 pyramidal neurons (Uylings et al. 1994). With this parameter set, model neurons were grown up to day 13.

Parameter Optimization

Finding a best fit of NETMORPH generated neuronal morphologies with an experimental data set requires a search strategy in a multi-dimensional parameter space

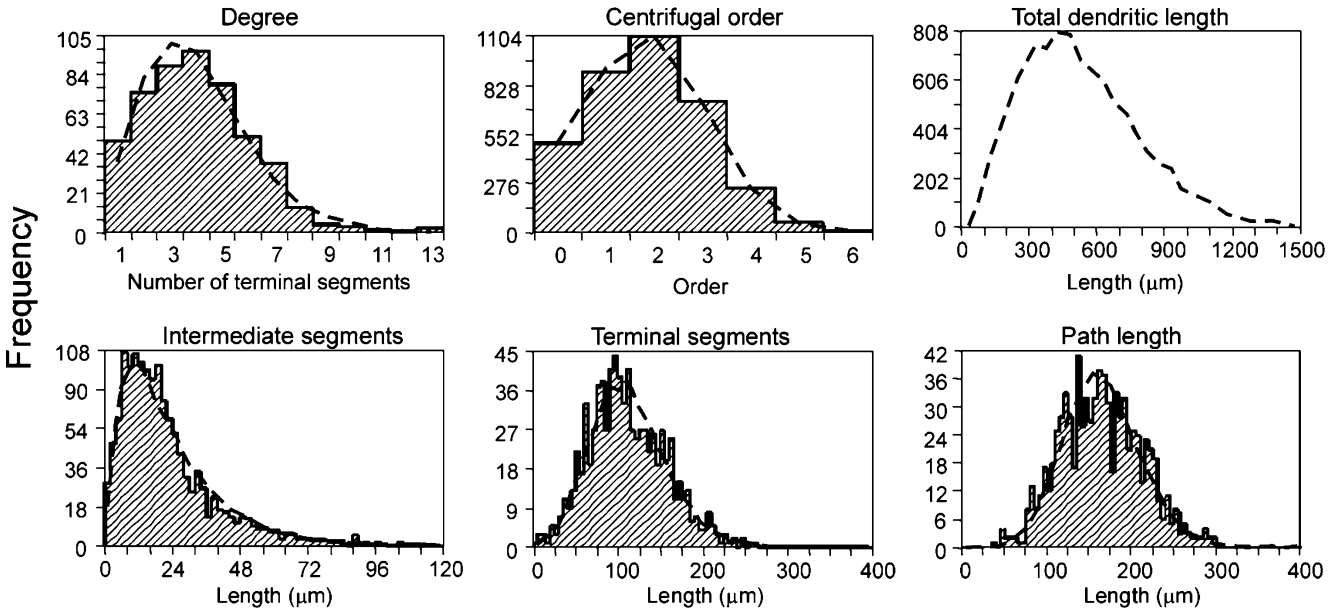

Fig. 4 Comparison of distributions of experimentally observed and model generated shape properties of day 18 S1-rat cortical layer 2/3 pyramidal cell basal dendrites. The model distributions were obtained for optimized model parameters taken from Van Pelt et al. (2001a). The experimental distributions were obtained from 3D reconstructions as described in Uylings et al. (1994). The different panels show the distributions of the number of terminal segments per dendritic tree (degree), centrifugal order of segments, total dendritic length (only predicted), length of intermediate, terminal segments and path length

(Table 1) and an iterative comparison of experimental and model shape properties. These properties can involve population means and standard deviations, but also the specific shapes of the distributions, as illustrated in Figs. 4 and 5. In the search strategy one can make use of the fact that some parameters in the model are directly related to shape properties of the branching patterns. For instance, parameter S predicts directly the mean asymmetry of the trees (Fig. 6). Thus an estimate of parameter S can be obtained from the mean tree asymmetry in the experimental data set. Parameters B and E are directly related to the shape of the terminal segment number distribution, as shown in Fig 7, in which the B-E parameter plane is mapped onto the plane of mean and standard deviation of the degree distribution. Thus an estimate of B and E can be obtained by plotting the mean and standard deviation of the experimental degree distribution in the parameter plane and deriving the coordinates of this point in the mapped B-E coordinate grid. The branching process governed by the parameters S, B, E, and τ fully determines the topological structure of the generated trees, as quantified by tree asymmetry, number of segments, and the distribution of segments versus centrifugal order, as well as their changes over developmental time. The metrical properties of the generated trees (e.g. segment length, path length), however, are determined by both the branching and the elongation process. For the optimization strategy it is therefore important to first optimize the branching parameters before optimizing the elongation parameters.

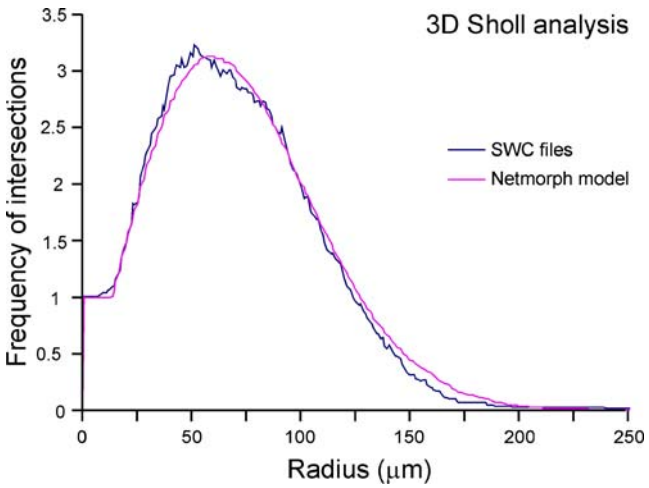

Fig. 5 3D-Sholl analysis of the basal dendritic trees of 25 reconstructed rat cortical layer 2/3 pyramidal neurons from the NeuroMorpho.org site (Markram), and of NETMORPH simulated neurons. The curves are normalized to have one intersection at short radii (i.e. one root segment)

In our growth model, newly formed daughter segments after a branching event are given an initial length. This assumption was needed to give the intermediate segment length distribution a modal shape, as shown in Fig. 4. Thus an estimate of the initial length parameters l_{in}-mn, l_{in}-sd can be obtained from the position of the peak in the experimental intermediate segment length distribution. The optimization of the elongation parameters (initial

Table 1 Growth model parameters in NETMORPH

parameter	description	related to
T	duration of growth	
S	order dependency in branching	mean tree asymmetry
B	time integral of baseline branching rate function D(t)	degree distribution
E	competition parameter in branching	degree distribution
τ	time constant in exponential function D(t)	degree growth curve
l_{in}-mn	initial length of daughter segments after branching	segment length
l_{in}-sd	standard deviation in initial length	segment length
ν-mn	mean elongation rate	segment length
ν-sd	standard deviation in elongation rate	segment length

length and elongation rates) involves for each parameter set a comparison of the experimental and model segment and path length distributions. The parameter search may be done manually, but can also be automated using a genetic algorithm to search for combinations of parameter values with optimal fits.

Use of NETMORPH Simulator

A simulation run of NETMORPH is based on a script, a text file that contains parameter identifiers with associated values specifying the duration, the time step, and other parameters required for the growth process. These include the model specifications and the various probability density functions from which random samples are to be drawn. The structure of the scripts, and the parameters that can be used to specify the growth process, are explained in the manual of NETMORPH (Koene et al. 2009).

Space and Position of Cell Bodies A number of spatial areas can be selected that constrain the placement of the cell bodies (Koene et al., 2009). The default area in 3D is a disc-shaped region (resembling a slice section of cortex), and the default area in 2D is a circle (resembling the environment of cultured neurons). In both cases, the default placement of somata is done randomly with a parameter for the minimum distance between adjacent soma centers.

Specification of Cell Types For each spatial area different morphological cell types can be selected. Each cell type model sets its own initial conditions and develops the morphological characteristics of that cell type. Soma diameters are drawn from a given normal distribution. The orientation of axon outgrowth at neuron placement may be specified, but is random by default. The initial lengths of axons and dendrites are zero by default. Cell type populations are specified either by their total number or by proportion, which by default are 80% pyramidal neurons and 20% interneurons (Koene et al. 2009). Morphological types are randomly distributed during cell placement.

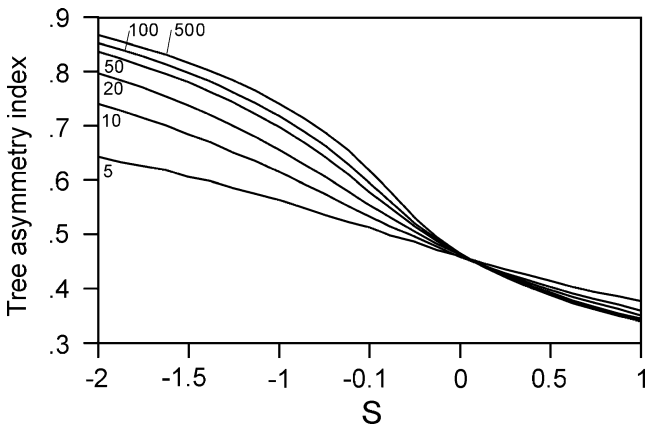

Fig. 6 Dependence of the mean tree asymmetry on the parameter S, which determines the order-dependency in branching. This relationship depends on the degree of the trees as indicated for the different curves

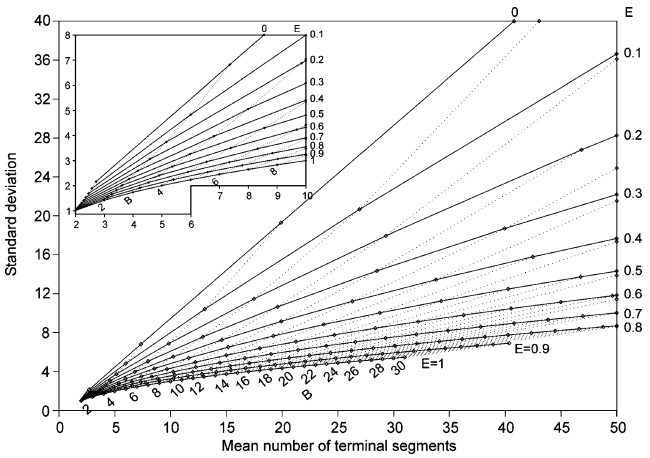

Fig. 7 Mapping of the ($B(T)$, E) space onto the (mean, SD) space of the terminal segment number distributions. Continuous lines connect (mean, SD) data points predicted for a particular value of parameter E. Dotted lines connect (mean, SD) data points predicted for a particular value of parameter B. The inset shows the mapping in more detail for small values of the mean and SD. A similar type of figure with other ranges can be found in Van Pelt and Uylings (2002)

Parameter Specification of Cell Types The dendritic outgrowth model has been developed for individual neuritic trees. Axons and dendrites are, obviously, different tree classes, but the dendritic trees themselves may also be subdivided into different tree classes. For instance, a pyramidal neuron consists of basal dendrites, apical main stem, apical tuft and oblique dendrites. Each of these tree classes requires separately optimized growth parameters.

Generation of Individual Neurons Neurons are grown during a specified period of development. At each time step Δt and for each growth cone, decisions are made for elongation, branching, redirection, etc. The stochastic nature of the simulator requires random sampling operations that use the various specified probability density functions (PDFs).

Examples of Model-Generated Dendritic Morphologies

Examples of NETMORPH generated dendritic morphologies were obtained by optimizing the model parameters to data sets of experimental reconstructions made available in the Neuromorpho.org website. Reconstructions of rat cortical layer 2/3 pyramidal neurons from Markram (see Wang et al. 2002) and from Svoboda (see Shepherd and Svoboda 2005) were downloaded in the form of .swc files. The data were analyzed with respect to several shape properties such as degree, asymmetry and segment lengths. A genetic algorithm was used to search for optimal model parameter values that reproduce these shape characteristics in the generated model dendrites. Examples of randomly generated neurons produced with these optimized parameter values are shown in Fig. 8a–d, along with examples of individual reconstructed neurons from the Neuromorpho.org site.

Figure 8e–g show examples of NETMORPH generated developing neurons at different ages. These examples are obtained by optimizing growth parameters to data sets of (Fig. 8e) rat lower layer 2/3 pyramidal cells from Markram (Wang et al. 2002); (Fig. 8f) rat layer 5 pyramidal cells from Staiger (Schubert et al. 2006), and (Fig. 8g) layer 4 basket cells from Markram (Wang et al. 2002).

For the above given examples it is important to note that optimization of model parameters was done using the data as provided in the database. That is, no correction was made for any distortion of the neuronal geometry (such as neurite tortuosity or length scales) as caused by slicing (cut endings) or tissue handling (e.g. tissue shrinkage).

Example of Axonal Morphologies

NETMORPH generated axonal morphologies were obtained by optimizing the model parameters to data sets from studies on the morphological development of in vitro rat cortical neurons (data of Ger Ramakers and Ellen Kampert; see Ramakers et al. (1998) for culturing methods). The morphology of the axonal branching patterns was quantified at various days of development up to 21 days in vitro (DIV). Briefly, primary cultures of dissociated cortical tissue were prepared from 18–19 day fetal rat cerebral cortex. Neurons were GFP transfected, and visualized at various days of development in vitro. Using a scanning stage, high-resolution confocal images were obtained from each stage position where an axon was present in the image field. These fields were subsequently brought into register in order to obtain an image of the full axonal branching pattern. Next, manual drawings were made of these axonal arborizations, which were entered into an image analysis procedure for segmentation of the different elements of the axon such as branch points and terminal tips. The segmentation step was followed by a quantification of the morphometric properties including the number of segments, and the length of intermediate and terminal segments. The developmental increase in the number of terminal segments and the total axonal length is shown in Fig. 9a and b, respectively. Note that the error bars (standard deviations) reflect both within and between individual culture variations. These growth patterns were also used in the optimization of the NETMORPH growth parameters, resulting in the values F=0.16; ν_0=45 μm/day; B_∞=17.38; E=0.39; S=0; τ=14 days. According to eqn (4) we have $B(t) = B_\infty\left(1 - e^{-t/\tau}\right)$ and at t=21 days, $B(21)=B_\infty(1-e^{-21/14})=$ 13.5. The growth curves from the NETMORPH generated axonal branching patterns are shown in Fig. 9 as continuous curves and individual data points (triangles). Both experimental and NETMORPH generated growth curves show nice agreement. Note that for each day of development different cultures were used with a varying number of neurons analyzed per culture (43, 36, 30, 17, 16, 4, 2, 3 and 2 for DIV 1, 2, 3, 5, 7, 9, 11, 14 and 21, respectively). These different sources of variance contribute substantially to the scatter of data points in Fig. 9b. A typical example of a NETMORPH generated axonal branching pattern at 21 days of development is shown in Fig. 10.

Locations of Synaptic Connections

Together with the development of neuronal morphology, NETMORPH also simulates the development of synaptic connectivity. In biological neuronal networks, axodendritic synapses can form where axonal and dendritic fibers are in sufficiently close proximity (Peters 1979; Stepanyants et al. 2004; Stepanyants and Chklovskii 2005).

Accordingly, NETMORPH searches for sites where pieces of axons and dendrites are separated from each other less than a given distance (see Fig. 11). This yields a

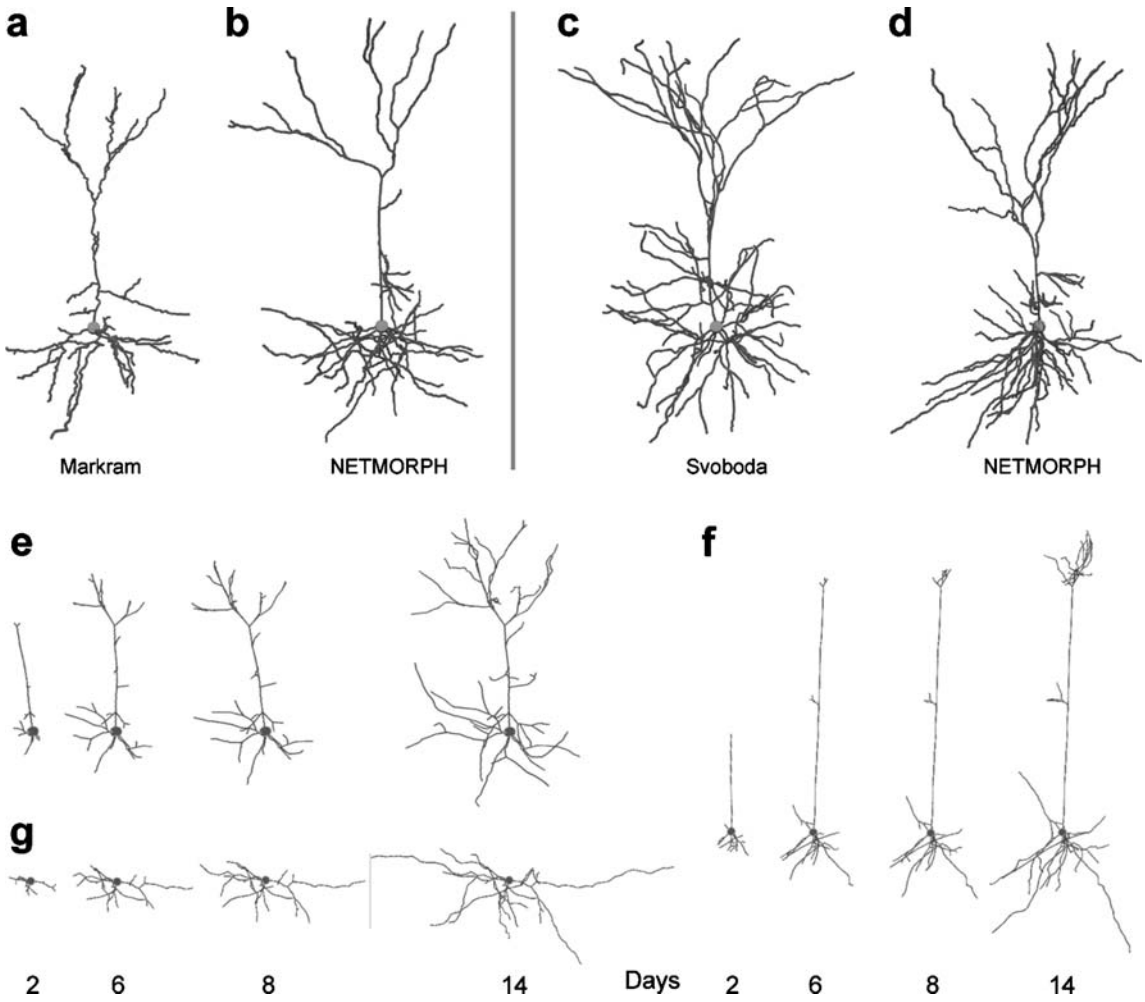

Fig. 8 (**a**–**d**) Comparison of reconstructed and NETMORPH generated dendritic morphologies. (**a**) A typical example from the Markram set of reconstructed rat cortical lower layer 2/3 pyramidal neurons, obtained from the Neuromorpho.org database. (**b**) A typical random NETMORPH generated neuron using a model parameter set optimized for the Markram data set in (**a**). (**c**) A typical example from the Svoboda set of reconstructed rat cortical upper layer 2/3 pyramidal neurons, obtained from the Neuromorpho.org database. (**d**) A typical NETMORPH generated neuron using a model parameter set optimized for the Svoboda data set in (**c**). (**e**–**g**) Growth of three model neurons at several days of development. The NETMORPH generated dendritic structures were obtained with model parameters optimized for three different cell groups, using reconstructed neurons from the Neuromorpho.org database of (**e**) rat lower layer 2/3 pyramidal cells from Markram, (**f**) rat layer 5 pyramidal cells from Staiger, and (**g**) layer 4 basket cells from Markram

set of candidate synaptic sites, each site being defined in terms of a specific location on a dendrite and a specific location on an axon. NETMORPH performs this search during the outgrowth process or, alternatively, at the end of simulated neuron growth. By default, one synapse is generated at each candidate site. Figure 12d gives an illustration of the locations of these synaptic sites (proximity criterion of 1 μm) in a developing network after 21 days of growth. The dendritic growth parameters used for this figure were F=0.39; ν_0= 12 μm/day; B_∞=4.75; E=0.5; S=0; τ=3.7 days.

Connectivity

An interesting anatomical aspect of the generated networks is their synaptic connectivity structure, which will be a function of axonal and dendritic morphologies. Network connectivity may be specified in terms of which neurons are connected; how the connectivity between neurons depends on the distance between their somata; and the multiplicity of the connections, i.e. the number of synaptic connections from a presynaptic to a postsynaptic neuron. Figure 12a–c show a developing network at different times of simulated development; the resulting synaptic locations at day 21 are depicted in Fig. 12d. Connection multiplicities are shown in Fig. 12e–f at different values of thresholding to focus on connections with at least a minimal number of synapses. Figure 13 shows graphs that depict the frequency of synapses at different radial distances from the somata (Fig. 13a,b) and the frequency of connections between neurons at different radial distances

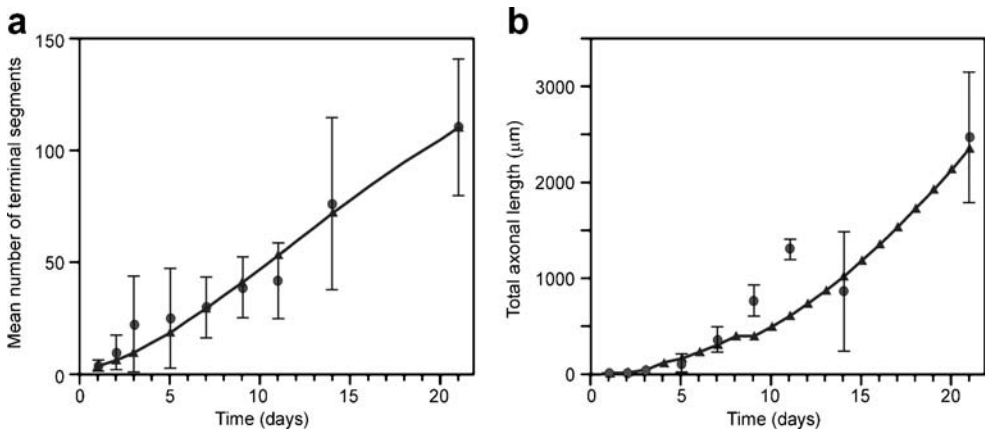

Fig. 9 Axonal development in mean (sd) number of terminal segments (**a**) and in total length of neurons cultured in vitro (bullets and error bars) (**b**). Continuous curves and triangles denote the growth of axons of NETMORPH generated neurons during a growth period of 21 days. Growth parameters were optimized to the morphology of experimental reconstructed axons of cultured neurons at the various developmental time points at which cultures were terminated (unpublished data of Ger Ramakers, and reconstructions by Ellen Kampert)

(Fig. 13c) in the same network after 21 days of simulated development. These preliminary model-based findings compare qualitatively well with empirical distributions (e.g., Le Bé et al. 2007; Hellwig 2000), showing a prevalence of connections at a specific range of distances (e.g., Sporns et al. 2004; Kaiser and Hilgetag 2007). These examples illustrate that NETMORPH can be used to study how connectivity distributions arise and how intrinsic geometric factors, such as the average distance between somata and elongation and branching rates, influence the shape of such distributions.

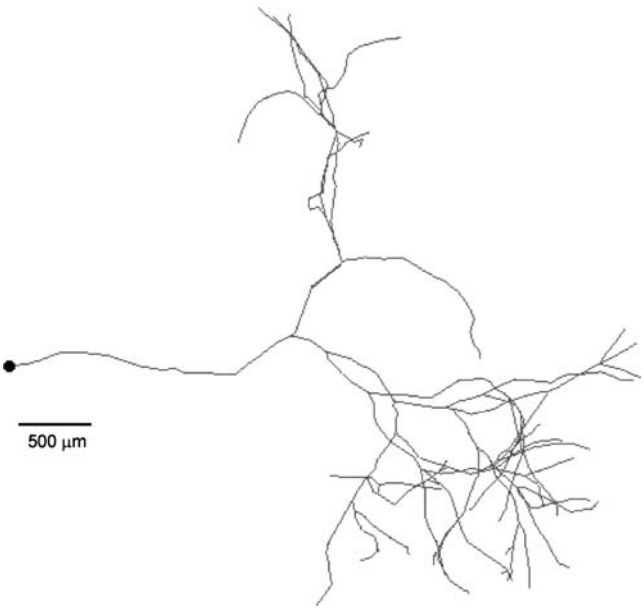

Fig. 10 Example of an axonal branching pattern at 21 days of development generated by NETMORPH. Growth parameters were optimized to experimental developmental data set of axon growth in tissue culture (unpublished data of Ger Ramakers)

Candidate synaptic sites are searched for on the basis of a proximity criterion. The number and location of synapses are therefore highly dependent on the morphological details of the axonal and dendritic arborizations, such as their tortuosity. The fine structure of dendrites and axons thus affect the resulting connectivity in the network. As a note of caution, it is important to realize that the staining process of the tissue prior to morphological reconstruction might affect this fine structure

A qualitative impression of a 3D network of cell bodies and axonal and dendritic fibers as well as synaptic locations is shown in Fig. 14. The visualization process involved solid rendering of the structures and raytracing (POV-Ray). In this example, all the axonal and dendritic segments have equal diameter.

NETMORPH Implementation

NETMORPH is implemented in object oriented C++. Simulations are initialized and run through a textual interface (script or command line). Simulation output comes in the form of textual reports, figures and animated

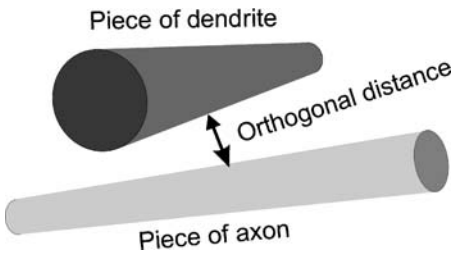

Fig. 11 Location of a candidate synapse when orthogonal distance between pieces of axon and dendrite is smaller than a criterion value

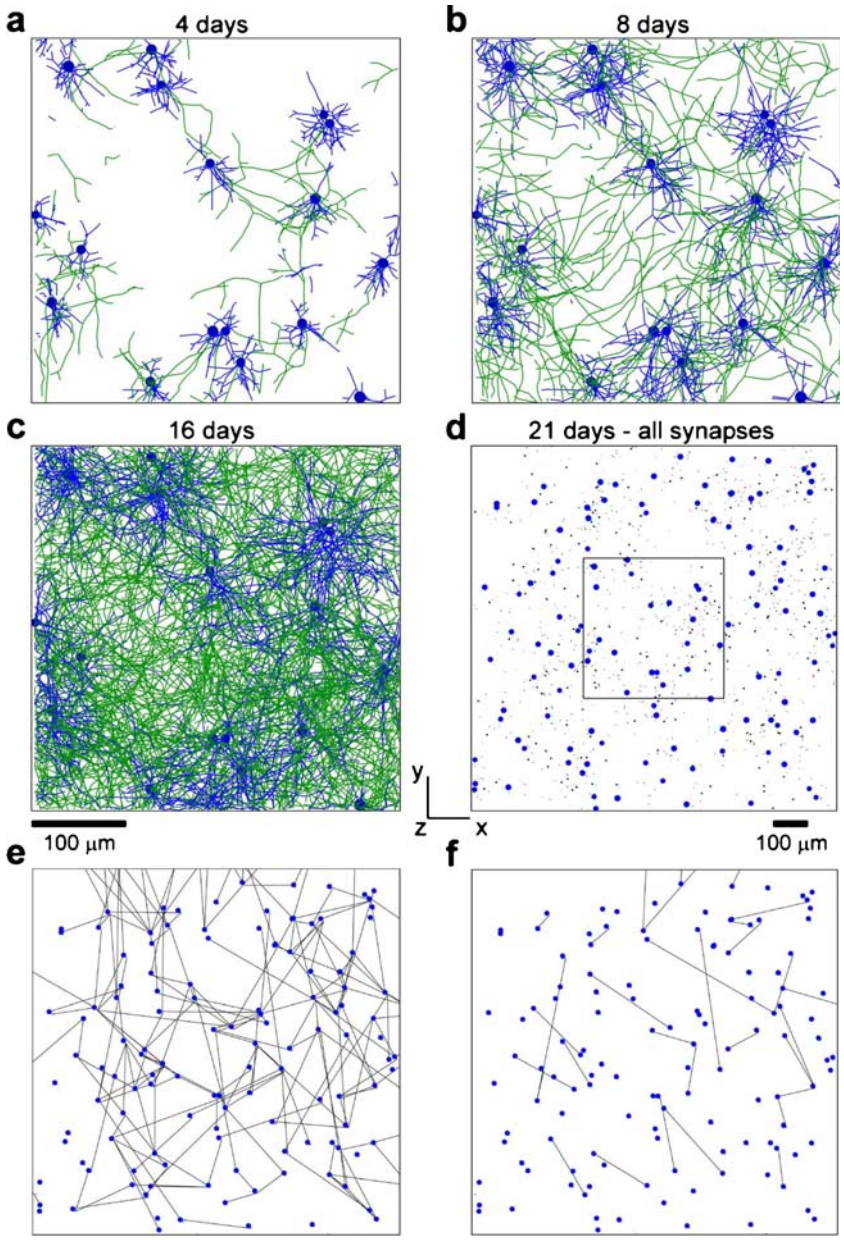

Fig. 12 **a–c** A 400μm x 400μm x 400μm volume excerpt of network development depicted in the x-y plane after 4, 8 and 16 days of development. Filled blue circles represent somata. Dendrite fibers are blue, axon fibers are green. (**d**): Synaptic sites (black dots) after 21 days of development in the same network excerpt, searched with a proximity criterion of 1 µm. Cell bodies are shown as filled blue circles. The rectangle indicates the volume excerpt of the network shown in the panels **a**–**c**. Note that some neurons do not appear at the depth ranges that are included in the volume excerpt. (**e**–**f**) Abstract connection diagrams of the network excerpt in (**d**) after 21 days of simulated development. The panels show all connections with multiplicity greater than (**e**) 25 % and (**f**) 50 % of the maximum multiplicity in the network. Connections retain their directionality, with the source neuron indicated by a small diagonal root line segment

sequences of development. The textual output of a simulation also lists simulation settings and an inventory of synapse formation. Several freely available programs are used for the post-processing that is needed to produce figures (*Octave*, *fig2dev*) and animated sequences (*convert*). The interface with NETMORPH is described in a manual (Koene et al. 2009). This manual informs the user about the installation and parameters of NETMORPH, and includes example scripts for the running of typical simulations. One of the options in NETMORPH is to export via text files the structure of the network, including the coordinates of all structural elements (such as somata, branch points, terminal points, continuation points, synapses). Another option is to export only abstracted connectivity, describing which neurons are connected and the multiplicity of their connections, but without the details of synapse location. We aim to provide standard output formats as used by programs such as NEURON (Hines and Moore 1993; Hines and Carnevale 1997).

Discussion

We have created a simulation framework for the generation of large scale neuronal networks with realistic neuronal morphologies. NETMORPH is a simulation tool that

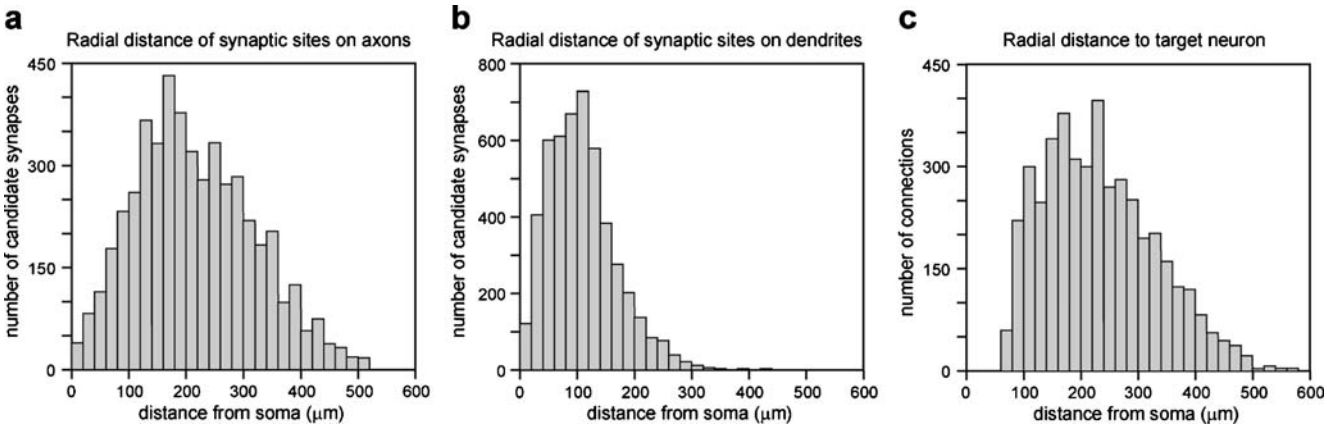

Fig. 13 Frequency by radial distance from pyramidal cell somata in bins of 20 μm for (**a**) presynaptic location on axons, (**b**) postsynaptic location on dendrites, and (**c**) connections from presynaptic to postsynaptic neurons, irrespective of the number of synapses

explicitly incorporates the developmental aspect of the generation of neuronal morphology. Networks are formed by the simultaneous outgrowth of many neurons in 3D space and connectivity emerges when axonal and dendritic branches come into sufficiently close proximity. In its present form, neurons grow out independently of each other. The morphological development of neurons and the formation of synaptic connectivity are modeled using sets of characteristic stochastic model functions and parameters. Simulations of network development enable analysis of emergent network connectivity. NETMORPH implements a neuronal outgrowth model in 3D based on earlier work of Van Pelt et al., with extensions for modeling branching angles and directions of outgrowth. These 3D morphological properties were validated using 3D Sholl analysis. This analysis captures, however, only one aspect of the 3D shape of neuronal arborizations, not fully covering shape properties such as neurite orientation (e.g. Uylings and Van Pelt 2002) and tortuosity. The generated neurons have been quantitatively compared with the morphology of experimentally reconstructed neurons obtained from the NeuroMorpho.org database with respect to a number of morphometric properties, further underscoring the morphological realism of the generated structures.

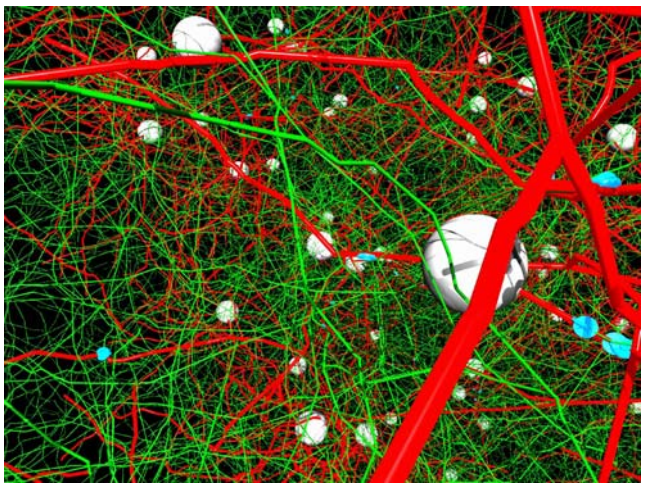

Fig. 14 A 3D view on a network generated by NETMORPH and visualized through solid rendering and raytracing (POVRAY). The figure gives an impression of how cell bodies (white), axons (green), dendrites (red) and synaptic connections (blue disks) are embedded in 3D space

The model is based on parametric stochastic functions for neurite outgrowth and branching. The functions have been designed so as to capture some basic biological principles of neuronal development, namely competition between growth cones for resources, dependence of branching probability on the growth cone's distance from the soma, and the inclusion of an exponentially decreasing baseline branching rate function. The parameter values optimized for particular cell types thus reflect and quantify these biological principles in a phenomenological manner. For instance, the requirement of a baseline branching rate function predicts that during the period of outgrowth the intracellular processes involved in branching exert an exponentially decreasing drive for branching (e.g., as the joint effect of the changes in expression of the many genes involved in dendritic branching, e.g., Jan and Jan 2003).

The 3D implementation of the neuronal growth model makes it possible to search for locations where dendritic and axonal segments are in close proximity. Taking these locations as candidate sites for synaptic connections provides an estimate of synaptic connectivity on pure geometrical grounds, since model neurons in NETMORPH grow out without interactions. The question to what extent such connectivity depends on the tortuosity of the neurites is a topic of further research. Network connectivity in NETMORPH is an emergent property arising from the geometry of independently outgrowing axons and dendrites. An interesting application therefore concerns investigating the complex relationship between neuronal

morphology and local and global patterns of synaptic connectivity (e.g. small-world connectivity).

NETMORPH as provided on our website (see Information Sharing Statement) is a working version with full functionality. We are continuously improving NETMORPH and its documentation and are currently working on a user-friendly graphical user interface. In addition, we intend to build an integrated software environment around NETMORPH (NetmorphLab) to offer the user an integrated set of neuroinformatics tools and facilities for databasing / datasharing, data analysis, data visualization, as well as computational modeling for studies of the morphology and function of neurons and neuronal networks.

The outgrowth model used in NETMORPH has so far mainly been used to generate dendritic morphologies. Further validation of model-generated axonal morphologies therefore remains necessary. NETMORPH is designed with a modular structure, such that it can accommodate further extensions and modifications, for example with respect to the model assumptions and specifications. The modularity concerns not only how morphological development is separated into different actions of the growth cone, but also the selection of the model functions for these actions, implemented in NETMORPH as model chains. In this respect, future extensions of the outgrowth model may also account for interactions of migrating growth cones with their local environments. For example, we are testing models in which outgrowing neurites are attracted to specific targets in their environment, (see Koene et al. 2009).

The neuronal networks generated by NETMORPH may provide realistic connectivity patterns that could be used in tools such as NEURON to simulate activity dynamics. In this respect, an interesting research question concerns the impact of activity-dependent outgrowth rules on the development of the neuronal network. Future extensions of NETMORPH will include tools to study the role of activity in neuronal morphogenesis and network development using detailed neuronal morphologies rather than abstract neuritic fields as in previous studies (Van Ooyen et al. 1995, 1996; Fields and Itoh 1996; Konur and Ghosh 2005). To do this, NETMORPH then needs to manage simultaneously both the slow processes of morphogenesis (days) and the fast processes of network activity (milliseconds).

Information Sharing Statement

The NETMORPH software and the NETMORPH manual are made available at http://www.neurodynamics.nl. This site also includes the NETMORPH model scripts and instructions for producing the results presented in this paper. We are continuously improving NETMORPH and its documentation.

Acknowledgment The development of the NETMORPH code by Dr. Randal Koene was supported by the Netherlands Organization for Scientific Research (Nederlandse Organisatie voor Wetenschappelijk Onderzoek) through the Program Computational Life Sciences grant CLS2003 (635.100.005) to Dr. Jaap van Pelt and Dr. Arjen van Ooyen, and by the EC Marie Curie Research and Training Network (RTN) NEURoVERS-it 019247. The validation of NETMORPH was additionally supported by the EU BIO-ICT Project SECO (grant 216593). The authors thank Nikos Green for contributing data sets of cultured neurons.

References

Aeschlimann, M. (2000). Biophysical models of axonal pathfinding. Ph.D. thesis, University of Lausanne.

Ascoli, G., & Krichmar, J. (2000). L-neuron: a modeling tool for the efficient generation and parsimonious description of dendritic morphology. *Neurocomputing, 32–33*, 1003–1011.

Ascoli, G., Krichmar, J., Nasuto, S., & Senft, S. (2001a). Generation, description and storage of dendritic morphology data. *Philosophical Transactions of the Royal Society of London B, 356*, 1131–1145.

Ascoli, G., Krichmar, J., Scorcioni, R., Nasuto, S., & Senft, S. (2001b). Computer generation and quantitative morphometric analysis of virtual neurons. *Anatomy and Embryology, 204*, 283–301.

Bamburg, J. (2003). Introduction to cytoskeletal dynamics and pathfinding of neuronal growth cones. *Journal of Histochemistry & Cytochemistry, 51*(4), 407–409.

Belmonte, M., & Bourgeron, T. (2006). Fragile x syndrome and autism at the intersection of genetic and neural networks. *Nature Neuroscience, 9*, 1221–1225.

Braitenberg, V., & Schütz, A. (1998). *Cortex: statistics and geometry of neuronal connectivity*. Berlin: Springer.

Butz, M., Lehmann, K., Dammasch, I., & Teuchert-Noodt, G. (2006). A theoretical network model to analyse neurogenesis and synaptogenesis in the dentate gyrus. *Neural Networks, 19*, 1490–1505.

da Costa, L. F., Manoel, E., Faucereau, J., Chelly, J., Van Pelt, J., & Ramakers, G. (2002). A shape analysis framework for neuromorphometry. *Network, 13*(3), 283–310.

Dityatev, A. E., Chmykhova, N. M., Studer, L., Karamian, O. A., Kozhanov, V. M., & Clamann, H. P. (1995). Comparison of the topology and growth rules of motoneuronal dendrites. *J. Comp Neurol., 363*, 505–516.

Douglas, R., & Martin, K. (2004). Neuronal circuits in the neocortex. *Annual Review of Neuroscience, 27*, 419–451.

Eberhard, J. P., Wanner, A., & Wittum, G. (2006). NeuGen: A tool for the generation of realistic morphology of cortical neurons and neuronal networks in 3D. *Neurocomputing, 70*(1–3), 327–342.

Fields, R., & Itoh, K. (1996). Neural cell adhesion molecules in activity-dependent development and synaptic plasticity. *Trends in Neurosciences, 19*, 473–480.

Gleeson, P., Steuber, V., & Silver, R. (2007). neuroConstruct: a tool for modeling networks of neurons in 3D space. *Neuron, 54*, 219–235.

Goldberg, D., & Burmeister, D. (1989). Looking into growth cones. *Trends in Neurosciences, 12*(12), 503–506.

Goodhill, J. G. (1998). Mathematical guidance for axons. *Trends in Neurosciences, 21*, 226–231.

Gordon-Weeks, P. R. (2000). *Neuronal Growth Cones*. Cambridge, United Kingdom: Cambridge University Press.

Graham, B., & Van Ooyen, A. (2004). Transport limited effects in a model of dendritic branching. *Journal of Theoretical Biology, 230*, 421–432.

Hellwig, B. (2000). A quantitative analysis of the local connectivity between pyramidal neurons in layers 2/3 of the rat visual cortex. *Biol. Cybern., 82*, 111–121.

Hely, T., Graham, B., & Van Ooyen, A. (2001). A computational model of dendrite elongation and branching based on map2 phosphorylation. *Journal of Theoretical Biology, 210*, 375–384.

Hentschel, H. G. E., & Van Ooyen, A. (1999). Models of axon guidance and bundling during development. *Proceedings of the Royal Society of London Series B, 266*, 2231–2238.

Hillman, D. (1979). Neuronal shape parameters and substructures as a basis of neuronal form. In F. Schmitt (Ed.), *The neurosciences, 4th study program* (pp. 477–498). Cambridge: MIT.

Hillman, D. E. (1988). Parameters of dendritic shape and substructure: intrinsic and extrinsic determination? In R. Lasek & M. Black (Eds.), *Intrinsic determinants of neuronal form and function* (pp. 83–113). New York: Alan R. Liss, Inc.

Hines, M., & Carnevale, N. (1997). The NEURON simulation environment. *Neural Computation, 9*, 1179–1209.

Hines, M., & Moore, J. (1993). A NEURON simulation program. In 23 rd Annual Meeting of the Society for Neuroscience.

Isbister, C., & O'Connor, T. (1999). Filopodial adhesion does not predict growth cone steering events in vivo. *Journal of Neuroscience, 20*, 2589–2600.

Jan, Y.-N., & Jan, L.-Y. (2003). The control of dendrite development. *Neuron, 40*, 229–242.

Kaiser, M., & Hilgetag, C. (2007). Development of multi-cluster cortical networks by time windows for spatial growth. *Neurocomputing, 70*, 1829–1832.

Kater, S. B. & Guthrie, P. B. (1990). Neuronal growth cone as an integrator of complex environmental information. In: Cold Spring Harbor Symposia on Quantitative Biology, vol. LV, Cold Spring Harbor, NY: Cold Spring Harbor Laboratory Press, 35.

Kiddie, G., McLean, D., van Ooyen, A., & Graham, B. (2005). Biologically plausible models of neurite outgrowth. In J. van Pelt, M. Kamermans, C. Levelt, A. van Ooyen, G. Ramakers, and P. Roelfsema, (Eds.), Development, dynamics and pathology of neuronal networks: from molecules to functional circuits, *Progress in Brain Research, 147*, 67–80. Elsevier.

Koene, R., Postma, F., de Ridder, S., Hoedemaker, S., van Pelt, J., & van Ooyen A. (2009) NETMORPH Manual. http://www.neurodynamics.nl/.

Konur, S., & Ghosh, A. (2005). Calcium signaling and the control of dendritic development. *Neuron, 46*, 401–405.

Kowalski, R. J., & Williams, R. J. (1993). Microtubule-associated protein 2 alters the dynamic properties of microtubule assembly and disassembly. *Journal Biological Chemistry, 268*, 9847–9855.

Lamoureux, P., Buxbaum, R. E., & Heidemann, S. R. (1998). Axonal outgrowth of cultured neurons is not limited by growth cone competition. *Journal of Cell Science, 111*, 3245–3252.

Larkman, A. U. (1991). Dendritic morphology of pyramidal neurons of the visual cortex of the rat I. Branching patterns. *Journal of Comparative Neurology, 306*, 307–319.

Larkman, A. U., Major, G., Stratford, K. J., & Jack, J. J. B. (1992). Dendritic morphology of pyramidal neurones of the visual cortex of the rat. IV: Electrical geometry. *Journal of Comparative Neurology, 323*, 137–152.

Le Bé, J.-V., Silberberg, G., Wang, Y., & Markram, H. (2007). Morphological, electrophysiological, and synaptic properties of corticocallosal pyramidal cells in the neonatal rat neocortex. *Cerebral Cortex, 17*, 2204–2213.

Letourneau, P., Kater, S., & Macagno, E. (eds). (1991). *The Nerve Growth Cone*. New York: Raven.

Luczak, A. (2006). Spatial embedding of neuronal trees modeled by diffusive growth. *Journal of Neuroscience Methods, 157*, 132–141.

Maskery, S. M., Buettner, H. M., & Shinbrot, T. (2004). Growth Cone Pathfinding: a competition between deterministic and stochastic events. *BMC Neuroscience, 5*, 22.

Nowakowski, R. S., Hayes, N. L., & Egger, M. D. (1992). Competitive interactions during dendritic growth: a simple stochastic growth algorithm. *Brain Research, 576*, 152.

Peters, A. (1979). Thalamic input to the cerebral cortex. *Trends in Neurosciences, 2*, 1183–1185.

Polinsky, M., Balzovich, K., & Tosney, K. (2000). Identification of an invariant response: Stable contact with schwann cells induces veil extension in sensory growth cones. *Journal of Neuroscience, 20*, 1044–1055.

Rall, W. (1959). Branching dendritic trees and motoneuron membrane resistivity. *Experimental Neurology, 1*, 491–527.

Ramakers, G. J. A., Winter, J., Hoogland, T., Lequin, M. B., Van Pelt, J., & Pool, C. W. (1998). Depolarization stimulates lamellipodia formation and axonal but not dendritic branching in cultured rat cerebral cortex neurons. *Development Brain Research, 108*, 205–216.

Samsonovich, A., & Ascoli, G. (2007). Computational models of dendritic morphology: From parsimonious description to biological insight. In M. Laubichler & G. Müller (Eds.), *Modeling Biology, Structures, Behaviors, Evolution* (pp. 91–113). Cambridge, Massachusetts: MIT.

Sánchez, C. J., Díaz-Nido, J., & Avila, J. (2000). Phosphorylation of microtubule-associated protein 2 (MAP2) and its relevance for the regulation of the neuronal cytoskeleton function. *Progress in Neurobiology, 61*, 133–168.

Scheff, S. W., Prince, D. A., Schmitt, F. A., DeKosky, S. T., & Mufson, E. F. (2007). Synaptic alterations in CA1 mild Alzheimer's disease and mild cognitive impairment. *Neurology, 68*, 1501–1508.

Schierwagen, A., & Grantyn, R. (1986). Quantitative morphological analysis of deep superior colliculus neurons stained intracellularly with HRP in the cat. *J Hirnforsch, 27*, 611–623.

Schubert, D., Kötter, R., Luhmann, H. J., & Staiger, J. F. (2006). Morphology, electrophysiology and functional input connectivity of pyramidal neurons characterizes a genuine layer Va in the primary somatosensory cortex. *Cereb Cortex, 16*(2), 223–36.

Segev, R., & Ben-Jacob, E. (2000). Generic modeling of chemotactic based self-wiring of neural networks. *Neural Networks, 13*(2), 185–199.

Senft, S., & Ascoli, G. (1999). Reconstruction of brain networks by algorithmic amplification of morphometry data. *Lecture Notes in Computer Science, 1606*, 25–33.

Shepherd, G. M., & Svoboda, K. (2005). Laminar and columnar organization of ascending excitatory projections to layer 2/3 pyramidal neurons in rat barrel cortex. *Journal of Neuroscience, 25*(24), 5670–5679.

Sporns, O., Chialvo, D., Kaiser, M., & Hilgetag, C. (2004). Organization, development and function of complex brain networks. *Trends in Cognitive Sciences, 8*, 418–425.

Stepanyants, A., & Chklovskii, D. (2005). Neurogeometry and potential synaptic connectivity. *Trends in Neurosciences, 28*(7), 387–394.

Stepanyants, A., Tamas, G., & Chklovskii, D. B. (2004). Class-specific features of neuronal wiring. *Neuron, 43*, 251–259.

Uylings, H., & Smit, G. (1975). Three dimensional branching structure of pyramidal cell dendrites. *Brain Research, 87*, 55–60.

Uylings, H. B. M., & van Pelt, J. (2002). Measures for quantifying dendritic arborizations. *Network: Computation Neural System, 13*, 397–414.

Uylings, H. B. M., Kuypers, K. & Veltman, W. A. M. (1978). Environmental influences on the neocortex in later life. In M. A. Corner (Ed.) *Maturation of the nervous system*. Progress in Brain Research, Vol 48, pp. 261–273. Elsevier, Amsterdam.

Uylings, H. B. M., Van Pelt, J., Parnavelas, J. G., & Ruiz-Marcos, A. (1994). Geometrical and topological characteristics in the dendritic development of cortical pyramidal and nonpyramidal neurons. In J. van Pelt, M. A. Corner, H. B. M. Uylings & F. H. Lopes da Silva (Eds.), *Progress in Brain Research, Vol. 102, the self-organizing brain: from growth cones to functional networks* (pp. 109–123). Amsterdam: Elsevier.

Van Ooyen, A., & Van Pelt, J. (1994). Activity-dependent outgrowth of neurons and overshoot phenomena in developing neural networks. *Journal of Theoretical Biology, 167*, 27–43.

Van Ooyen, A., & Van Pelt, J. (1996). Complex periodic behavior in a neural network model with activity-dependent neurite outgrowth. *Journal of Theoretical Biology, 179*, 229–242.

Van Ooyen, A., Van Pelt, J., & Corner, M. (1995). Implications of activity dependent neurite outgrowth for neuronal morphology and network development. *Journal of Theoretical Biology, 172*, 63–82.

Van Ooyen, A., Pakdaman, K., Houweling, A., Van Pelt, J., & Vibert, J.-F. (1996). Networks connectivity changes through activity-dependent neurite outgrowth. *Neural Processing Letters, 3*, 123–130.

Van Ooyen, A., Graham, B., & Ramakers, G. (2001). Competition for tubulin between growing neurites during development. *Neurocomputing, 38–40*, 73–78.

Van Pelt, J., & Uylings, H. (1999). Modeling the natural variability in the shape of dendritic trees: Application to basal dendrites of small rat cortical layer 5 pyramidal neurons. *Neurocomputing, 26–27*, 305–311.

Van Pelt, J., & Uylings, H. (2002). Branching rates and growth functions in the outgrowth of dendritic branching patterns. *Network: Computational Neural Systems, 13*, 261–281.

Van Pelt, J., & Uylings, H. (2003). Growth functions in dendritic outgrowth. Brain and Mind, 4:51–65. In A. van Ooyen, (Ed.), Modeling Neural Development, 75–94. Cambridge, MA: MIT Press.

Van Pelt, J., & Uylings, H. B. M. (2005). Natural variability in the geometry of dendritic branching patterns. In: G. N. Reeke, R. R. Poznanski, K. A. Lindsay, J. R. Rosenberg, & O. Sporns (Eds.), *Modeling in the Neurosciences: From Biological Systems to Neuromimetic Robotics*. CRC Press, 2005, pp. 89–115.

Van Pelt J. and Uylings H.B.M. (2007) Modeling neuronal growth and shape. In Modeling Biology—Structures, Behaviors, Evolution, Manfred D. Laubichler and Gerd B. Müller (Eds). The MIT Press, 2007, Cambridge, pp. 195–215.

Van Pelt, J., Uylings, H. B. M., Verwer, R. W. H., Pentney, R. J., & Woldenberg, M. J. (1992). Tree asymmetry—a sensitive and practical measure for binary topological trees. *Bulletin of Mathematical Biology, 54*, 759–784.

Van Pelt, J., Dityatev, A. E., & Uylings, H. B. M. (1997). Natural variability in the number of dendritic segments: Model-based inferences about branching during neurite outgrowth. *Journal of Comparative Neurology, 387*, 325–340.

Van Pelt, J., Van Ooyen, A., & Uylings, H. B. M. (2001a). Modeling dendritic geometry and the development of nerve connections. In: De Schutter E (Ed.), Cannon RC (CD-ROM) Computational Neuroscience: Realistic modeling for experimentalist, Chapter 7, CRC Press. pp 179–208.

Van Pelt, J., Van Ooyen, A., & Uylings, H. (2001b). The need for integrating neuronal morphology databases and computational environments in exploring neuronal structure and function. *Anatomy and Embryology, 204*, 255–265.

Van Pelt, J., Schierwagen, A., & Uylings, H. B. M. (2001c). Modeling dendritic morphological complexity of deep layer cat superior colliculus neurons. *Neurocomputing, 38–40*, 403–408.

Van Pelt, J., Graham, B., & Uylings, H. (2003). Formation of dendritic branching patterns. In A. van Ooyen (Ed.), *Modeling neural development* (pp. 75–94). Cambridge, Massachusets: The MIT.

Van Veen, M. P., & Van Pelt, J. (1993). Terminal and intermediate segment lengths in neuronal trees with finite length. *Bulletin of Mathematical Biology, 55*, 277–294.

Wang, Y., Gupta, A., Toledo-Rodriguez, M., Wu, C. Z., & Markram, H. (2002). Anatomical, physiological, molecular and circuit properties of nest basket cells in the developing somatosensory cortex. *Cerebral Cortex, 12*(4), 395–410.

Zubler, F., & Douglas, R. (2008) CX3D: a java package for simulation of cortical development in 3D. Frontiers in Neuroinformatics. Conference Abstract: Neuroinformatics 2008. doi:10.3389/conf.neuro.11.2008.01.127.